Materials and Design 173 (2019) 107761

Contents lists available at ScienceDirect

Materials and Design

journal homepage: www.elsevier.com/locate/matdes

Analysis and reduction of wrinkling defects for tube-hydroforming magnesium alloy components at elevated temperatures

T.F. Kong *, X.Z. Lu, L.C. Chan

Department of Industrial and Systems Engineering, The Hong Kong Polytechnic University, Hung Hom, Kowloon, Hong Kong, China

HIGHLIGHTS

- A collet-type device was used to reduce wrinkling defects in tube-hydroforming of Mg alloy AZ31B at elevated temperatures.
- Effects of material temperature and properties on the wrinkling defects during tube-hydroforming were analysed theoretically.
- Effects of die-core temperature and pre-heating time on wrinkling occurrence and wall thinning were studied by FE simulation.
- The most satisfactory barrel-shaped component was hydroformed at die-core temperature ≈ 350 °C and pre-heating time ≈ 10 s.
- A subsequent wrinkle-free bike-frame component was hydroformed successfully using the same approach and proposed tool design.

GRAPHICAL ABSTRACT

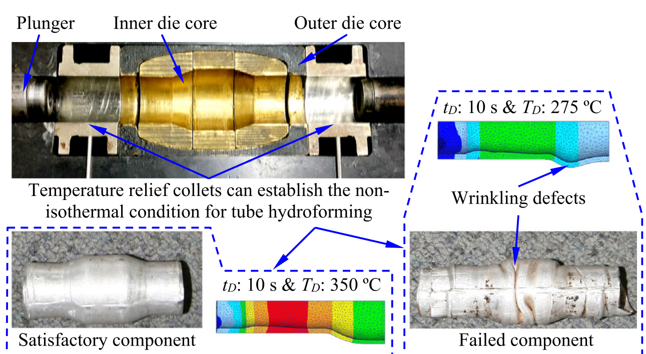

ARTICLE INFO

Article history:
Received 27 December 2018
Received in revised form 1 March 2019
Accepted 23 March 2019
Available online 25 March 2019

Keywords:
Tube hydroforming
Wrinkling
Elevated temperatures
Magnesium alloy
Tool design
Non-isothermal condition

ABSTRACT

Wrinkling defects commonly occur in tube hydroforming (THF) magnesium (Mg) alloy at elevated temperatures when the tube-end and axial-feeding regions of the workpiece are overheated. Most previously proposed methods for preventing such defects have been applied at room temperature and restricted by several limitations. Therefore, this paper presents a breakthrough in tool design through the appropriate control of temperature distribution of the Mg alloy AZ31B tubular material to minimise the wrinkling defects in THF at evaluated temperatures. The proposed cost-effective, simple and user-friendly collet-type device design was able to provide a non-isothermal condition for THF within an appropriate pre-heating time after die closing. An axisymmetric barrel-shaped component was taken as a prime example to demonstrate the methodology, in which various thermal potential differences between the axial-feeding and deformation regions were investigated using finite-element (FE) simulation so as to evaluate the wrinkling effects under various non-isothermal conditions. The results showed that the most satisfactory component could be obtained when the average temperatures of axial-feeding and deformation regions were around 240 and 330 °C, respectively. Subsequently, with the same approach, a wrinkle-free non-axisymmetric tubular bike-frame component was hydroformed successfully as a more realistic and practical application example.

* Corresponding author.
E-mail address: tf.kong@polyu.edu.hk (T.F. Kong).

https://doi.org/10.1016/j.matdes.2019.107761

1. Introduction

Hollow structural component with a complex variable cross-section are usually produced by sheet metal forming/stamping of separate simple parts, which can be welded back together subsequently [1,2]. Such method has the advantages of being able to produce large-sized and complex-shaped hollow components, however, this involves multiple operations resulting in lower productivity, and meanwhile increasing the tooling, assembly, and material preparation costs [3]. Tube hydroforming (THF) process, which makes use of a pressurised fluid as the forming medium to bulge tubular metals into the desired shapes, is believed to be an appropriate alternative method for industrial applications [4]. The tubular-structural components can be produced efficiently by this one-step process with lower tooling cost, fewer secondary operations, and tighter tolerances [5,6]. Thus, this manufacturing process is recognized as the most promising technology to produce high-quality tubular frame structural components. It is also beneficial for the optimisation of vehicle frame design to achieve lightweight, superior strength, better structural integrity, more stable skeleton for the power-train and suspension as well as more flexible component geometry, replacing the current practice in developing areas by using traditional stamping and welding processes for manufacturing most of the existing automotive components [7,8].

Owing to good plasticity and formability as well as an affordable price, ferrous materials such as stainless steel and carbon steel are the most widely used materials for THF process. The hydroformed steel products always attract much attention in automotive structural components such as exhaust system, suspension frames, cross members and engine cradles [9,10]. With the increasing need of lightweight to reduce fuel and energy consumptions in recent years, light metals such as aluminium (Al) alloy, magnesium (Mg) alloy and titanium (Ti) alloy are now led to the wide applications in the automotive, bike, aircraft, and aerospace industries due to their lightweight, higher specific strength and stiffness structures [11–14]. However, it is relatively difficult to deform these light metals into the desired shapes at room temperature. In feasible practice, the forming processes can be carried out at certain elevated temperatures to achieve the higher formability. By analysing the effects of temperature, blank holding force and lubrication on the deep drawing formability of Mg alloy sheet AZ31, Zhang et al. [15] concluded that the limit drawing ratio up to 2.6 can be achieved at a forming temperature ranging from 105 to 170 °C. Tari et al. [16] investigated the effect of temperature and temperature gradient on the formability of Mg alloy AZ31B sheet, and concluded that the formability was improved significantly with increasing temperature and introducing non-isothermal conditions within a proper process window. Tari and Worswick [17] studied the flow stress behaviour of Mg alloy AZ31B at elevated temperatures at both isothermal and non-isothermal conditions by using the Cowper–Symonds hardening model and modified Nadai model respectively.

It can be seen that the increase in temperature is crucial for improving the formability of light metal alloys. Therefore, various tooling setups and heating approaches have been proposed to accomplish the THF process at elevated temperatures, in which the workpieces or specimens were usually heated by thermal conduction from the contact surfaces of warm or hot forming dies and axial-feeding plungers. Yi et al. [18] developed a heating system which combined an induction coil and a heating element for the warm hydroforming of lightweight alloys, thus a uniform temperature distribution of the tube specimen was achieved. Liu et al. [19] proposed a concept of non-uniform temperature field in the warm hydroforming process, i.e., lower temperature in the feeding zone and higher temperature in the forming zone. Hence, the thickening of the feeding zone was alleviated and, as well, the thickness uniformity of the component was improved. The control of temperature distribution in the workpiece for THF was more significant than it was for other forming processes carried out at isothermal conditions. The overheating at the tube-end and axial-feeding regions caused the over-softening of those regions, at which, the plungers were incapable providing a proper sealing, as shown in Fig. 1. This caused the leakage of forming media such as thermal-resistant oil and inert gases, and subsequently the decline of internal pressure. Consequently, as illustrated in Fig. 2, wrinkling defects occurred at that over-softened region, when the internal pressure (p_i) was smaller than the radial stress (σ_r^z) generated by the axial stress (σ_z), which fed the material to the deformation region of the die cavity.

Some experimental methods have been proposed to overcome the sealing and wrinkling problems in THF. Yang and Guo [20] analysed two main sealing mechanisms used in THF, i.e., sealing wedge expansion and sealing by ironing, and proposed an experimental sealing tooling by making use of urethane expansion plugs, binding bolts and locked nuts for THF with large contracting in the axial direction.

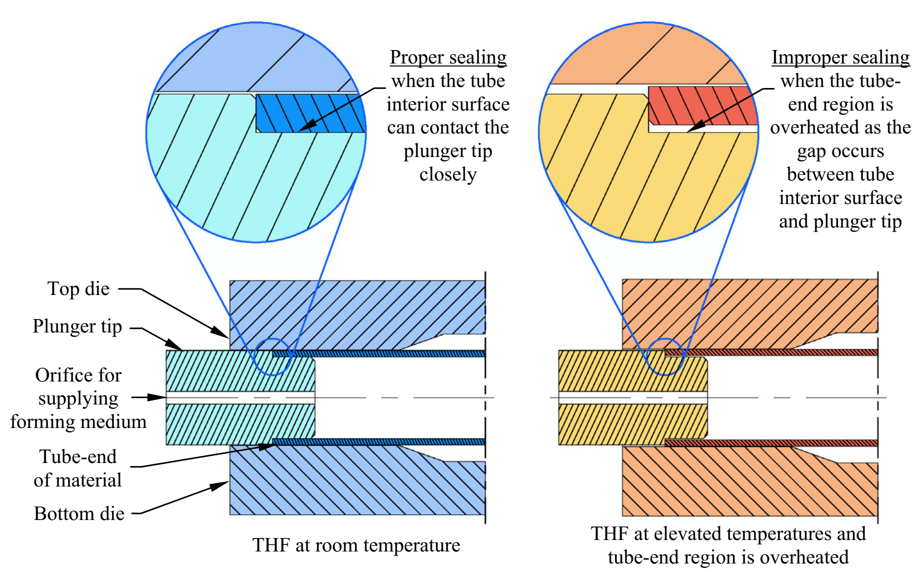

Fig. 1. The sealing conditions at the plunger tips in THF at room and elevated temperatures.

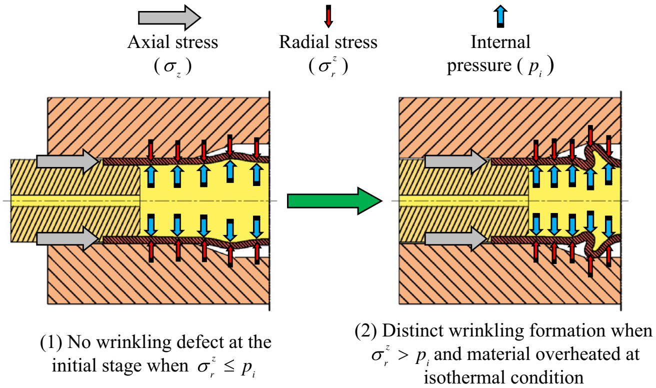

Fig. 2. The formation of wrinkling defects due to material softening at the axial-feeding region as the radial stress larger than the internal pressure.

Abedrabbo et al. [21] improved the sealing performance of THF by incorporating a Teflon ring and a high-pressure polymeric O-ring to the tip of the end-feed actuator. Park et al. [22] developed a novel sealing system composed of an additional cylindrical die spring, cylindrical sleeve and filleted plunger tip to prevent leakage of the forming media. However, such sealing systems were only tested at room temperature. Their configurations were quite complicated and might limit the maximum stroke of axial-feeding displacement. In terms of theoretical analysis, Liu et al. [23] proposed an analytical model based on an energy method using the energy conservation law to inhibit wrinkling in the thin-walled THF. The results showed that the increase of material strength coefficient (K) or the decrease of material hardening exponent (n) in the Hollomon hardening law could improve the wrinkle-resistant ability of tubular materials. This also suggested that the sufficient strength of the material at the axial-feeding regions, which would be fed to the deformation region, should be retained. Although the study only performed the cold THF with ferrous metals, the theoretical concept could be applied to the process and tooling design of THF light metals such as Mg alloy at elevated temperatures.

This paper presents a breakthrough in tool design through the appropriate control of the temperature distribution of Mg alloy AZ31B tubular material to minimise wrinkling defects in THF at evaluated temperatures. An axisymmetric Mg alloy barrel-shaped component was taken as a prime example to demonstrate the tool design concept and methodology. Various thermal potential differences between the axial-feeding regions and deformation region were investigated using finite-element (FE) simulation to analyse the wrinkling effects at various die temperature distributions. It was planned that, eventually, the THF process of a non-axisymmetric tubular Mg alloy AZ31B bike-frame component could verify this concept via the practical application.

2. Wrinkling effect in THF at elevated temperatures

As mentioned in the previous section and illustrated in Fig. 2, in the THF process, the material at the tube-end and axial-feeding regions under the die constraints, basically the occurrence of wrinkling effect, can be expressed as:

$$\sigma_i = p_i - \sigma_r^z \le 0 \tag{1}$$

where σ_i is the interfacial stress acted on the tubular workpiece material. To avoid the wrinkling defects, the value of σ_i cannot be a negative number.

On the other hand, at the bulging and deformation region, the additional radial stress portion (σ_r^θ) is required for the plastic deformation and should be taken into account in the wrinkling criterion model [23]. Thus, the updated equation expressing the occurrence of wrinkling effect in THF was:

$$\sigma_i = p_i - \sigma_r^z - \sigma_r^\theta \le 0 \tag{2}$$

The control of the internal pressure (p_i) and the radial stress (σ_r^z) generated by the axial stress (σ_z) can be implemented by the hydroforming machine, whereas the radial stress portion (σ_r^θ) is mainly dependent upon the hoop stress (σ_θ) of tubular material with varied flow stresses, which can be influenced by the elevated temperature (T). When $\sigma_i = 0$ or $p_i = \sigma_r^z + \sigma_r^\theta$, that internal pressure (p_i) is defined as the critical wrinkling pressure (p_c). According to the theory of elastic-plastic stability, p_c can be calculated by using the energy method [24] and stated as:

$$p_c = \frac{3(E_0 - E_w)}{2k_1 \delta L w} + \sigma_\theta \frac{2t}{D} \tag{3}$$

where E_0 and E_w are the strain energies in a perfect cylindrical surface and a wrinkled surface, respectively, L is the tube length, w is the circumferential arc width of a small-piece cylindrical surface, D is the tube outer diameter, and t is the tube wall thickness, δ is the maximum wrinkle amplitude that is perpendicular to the direction of the axial feeding displacement (u_z) and can be written as:

$$\delta = \frac{\sqrt{2}L}{\pi}\sqrt{1 - \left(\frac{L - 2u_z}{L}\right)^2} \tag{4}$$

k_1 is the equivalent factor as:

$$k_1 = \frac{\sin^{-1}\dfrac{\sqrt{D^2 - (D-\delta)^2}}{D} \times D^2 - (D-\delta)\sqrt{D^2 - (D-\delta)^2}}{2D\delta \sin^{-1}\dfrac{\sqrt{D^2 - (D-\delta)^2}}{D}} \tag{5}$$

The Mg alloy AZ31B is a growing light metal of selection for automotive and aircraft applications, but usually needs to be formed at elevated temperatures around 200–400 °C to improve the formability because the pyramidal plane of its hexagonal close-packed (HCP) crystal structure can be operated by thermal activation [25,26]. Therefore, the Mg alloy AZ31B was chosen as the specimen material in this study, and its forming temperatures of the THF trials were set as 275, 300, 325 and 350 °C. A modified Fields-Backofen constitutive equation proposed by Chan and Lu [27], taking the thermal softening effect into consideration [28], was employed to describe the thermal deformation behaviour of the Mg alloy AZ31B, that is:

$$\overline{\sigma} = C_1 \overline{\varepsilon}^n \dot{\overline{\varepsilon}}^m \exp(C_2/T) \tag{6}$$

where $\overline{\sigma}$ is the effective (flow) stress, $\overline{\varepsilon}$ is the effective strain, $\dot{\overline{\varepsilon}}$ is the effective strain rate, C_1 is the strength coefficient, and C_2 is the thermal softening coefficient. The work-hardening behaviour is described by the strain-hardening exponent n and the strain rate sensitivity exponent m.

In each THF process, it is assumed that the ratio of hoop stress to axial stress is the constant stress condition and expressed as:

$$\alpha = \frac{\sigma_\theta}{\sigma_z} \tag{7}$$

And thus the effective strain through the axial strain (ε_z) can be written as:

$$\overline{\varepsilon} = c\varepsilon_z \tag{8}$$

where

$$c = -\sqrt{\frac{2}{3}\left(1 + \frac{(1+\alpha)^2 + (2\alpha-1)^2}{(2-\alpha)^2}\right)} \tag{9}$$

and

$$\varepsilon_z = \ln\left(\frac{L-2u_z}{L}\right) \tag{10}$$

According to the analytical model [23], the critical wrinkling stress (σ_c) at the transit axial-feeding displacement (u_z/L) can be determined by:

$$\sigma_c = C_1\dot{\bar{\varepsilon}}^m \exp(C_2/T)\sqrt{\frac{2}{(1+\alpha^2+(1-\alpha)^2}}(c\varepsilon_z)^n = \frac{D(p_c - A\times B)}{2\alpha t} \tag{11}$$

where

$$A = \frac{3k_1C_1\bar{\varepsilon}^n\dot{\bar{\varepsilon}}^m \exp(C_2/T)t}{2(n+1)\delta} \tag{12}$$

and

$$B = \frac{\pi}{4}c\varepsilon_z{}^{n+1} - \frac{2}{L}\left(\frac{t}{\sqrt{3}}\right)^{n+1}\left\{2 + \frac{1+t}{[2\pi/(L-2u_z)]^2\delta}\right\}^{-n}\tan^{-1}\left\{\frac{[2\pi/(L-2u_z)]\delta}{2}\right\}\left(1+\frac{L^2}{W^2}\right)^2 \tag{13}$$

The critical wrinkling stress (σ_c) is therefore influenced by the material flow stress properties (i.e., C_1, C_2, m and n), effective strain rate ($\dot{\bar{\varepsilon}}$), elevated temperature (T), stress conditions (α), and axial strain (ε_z). The effect of α on $\sigma_c$was investigated by previous researchers [23]. Under the same internal pressure (p_i), an increase of αvalue could increase the σ_c that also reduced the occurrence of wrinkling effects. In addition, the positive value of α caused by the compression hoop stress could improve the tube stability.

In this study, the effect of elevated temperature (T) was included in the critical-wrinkling-stress equation. An axisymmetric barrel-shaped component shown in Fig. 3, was taken as a prime example. Based on the component geometry and the flow-stress parameters of Mg alloy AZ31B, the relationship among the critical-wrinkling-stress (σ_c), internal pressure (p_i), elevated temperature (T) and strain rate ($\dot{\bar{\varepsilon}}$) was obtained. Fig. 4 shows the effects of T on σ_c at $\dot{\bar{\varepsilon}}$, where the other material parameters were taken as $C_1 = 4$ MPa, $C_2 = 2000$ K, $n = 0.1$ and $m = 0.03$. When the temperature increased, the critical wrinkling stress decreased so that the wrinkling defects occurred easily. On the other hand, the critical wrinkling stress was increased gradually by increasing the strain rate.

3. Tool design for non-isothermal THF

For THF Mg alloy components, an elevated forming temperature can definitely improve the material formability, whereas it probably increases the risk of wrinkling occurrence due to the lower critical wrinkling stress. Therefore, the method or approach of temperature control and determination for the tubular workpiece material is very significant. Traditionally, as the simplest way to maximise elongation of the material, the cold or preheated workpiece is usually placed into a high-temperature die core like the intuitive design shown in Fig. 5a, then the workpiece can be heated directly by radiation and thermal conduction with contact heat transfer from the die-cavity surface up to the desired temperature that the die material and forming media can withstand. In this situation, the temperature of the whole workpiece is distributed evenly and same as that of the die cavity, which is so-called an isothermal forming condition. In this condition, the process design and control are straightforward as the thermal potential differences among various regions of the workpiece are disregarded. However, the flow of tubular material, as well as its contact-friction against the die-cavity surface, is varied when the temperature is rising, particularly for the tube-end and axial feeding regions where the tubular workpiece closely contacts the die-cavity surface with an increase of frictional coefficient acted. This may restrict the material feeding to the deformation region intensely, and the material wall thickness near the tube end is butted or thickened by the compression axial stress.

In order to facilitate the axial feeding of tubular material and investigate how to reduce the wrinkling defects in the complicated non-isothermal THF condition, a breakthrough design of the THF tool (i.e., the die) was proposed, with the view of attaining the more reasonable temperature distribution of the tubular workpiece so as to mitigate the overheating problem at the axial-feeding regions. Fig. 5b shows the tool configurations and their materials, in which a pair of temperature relief collets were the portions to provide the die constraint for axial-feeding and separated from the deformation region of the die cavity. Before the start of THF process, the collets and tubular workpiece stayed outside the forming die and remained at room temperature. Both of them were then placed into the isothermal die and heated together for a short period of time. The collets were made of austenitic stainless steel with a much lower thermal conductivity compared to the Mg alloy (i.e., 20 W/m·K vs. 96 W/m·K), also the collet grooves acted as insulation to slow down the heat transfer from the die. This could generate a thermal potential difference within the tubular workpiece that the temperature of the axial-feeding region was lower than that of the deformation region. This was a breakthrough idea to provide the non-isothermal condition effectively for reducing wrinkling defects/effects during THF at elevated temperatures within an appropriate pre-heating time after die closing.

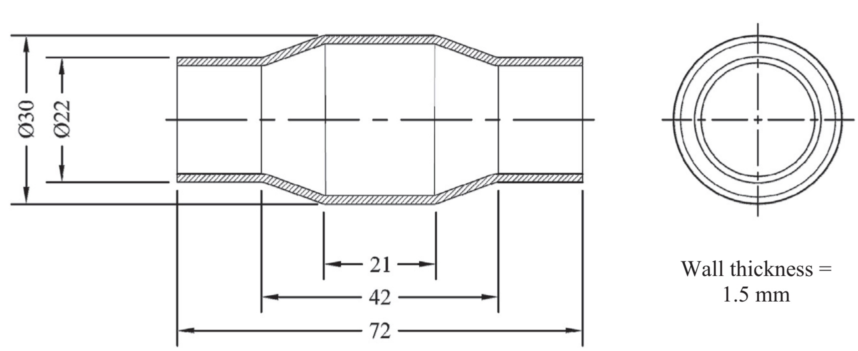

Fig. 3. The axisymmetric barrel-shaped component.

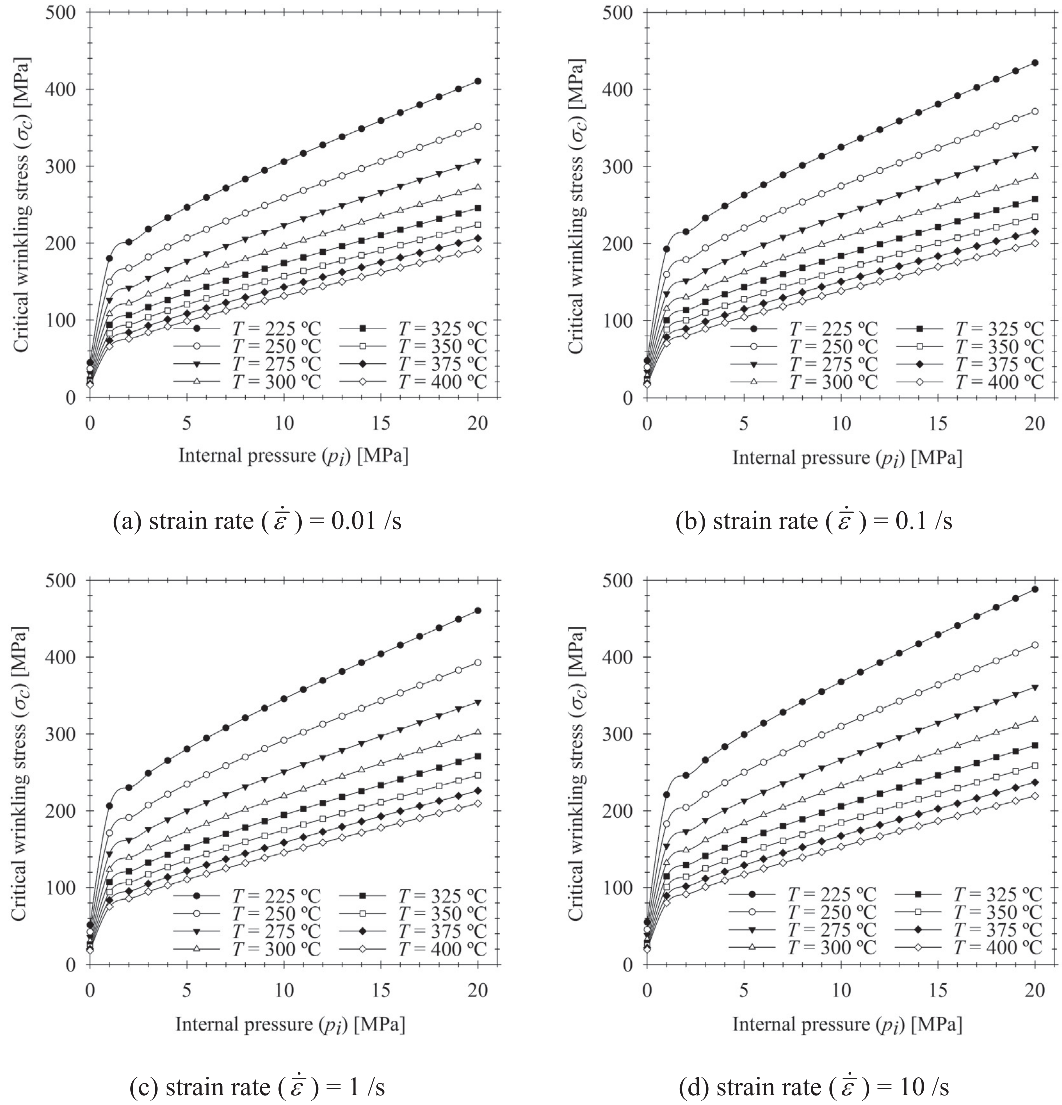

Fig. 4. The relationship among the critical-wrinkling-stress (σ_c), internal pressure (p_i), elevated temperature (T) and strain rate ($\dot{\varepsilon}$) in THF.

4. Process simulation and experimental work

The critical-wrinkling-stress equation implies that a higher temperature of the workpiece material would cause wrinkling defects easily in THF under the isothermal condition. However, the non-isothermal THF condition was more complicated because it involved instantaneous changes of stress states, workpiece-die interface friction, and material flow-stress properties, when the temperature distribution of the workpiece was varied by heat transfer from multi-material die components with their different thermal conductivities and heat capacities. In order to obtain the related findings from such a complicated case, the wrinkling effects were investigated against various thermal potential differences between the axial-feeding and deformation regions of the AZ31B tubular material with the proposed THF die configuration using finite-element (FE) simulation. Fig. 6 shows the 3D model of THF setup for FE simulation, which was modelled using the commercial software DEFORM-3D. In order to improve the accuracy of heat-transfer and material-flow predictions, all geometric models were simplified to one-eighth of the original 3D models that speeded up the computation and increased the number of tetrahedral meshes for each volume.

The Mg alloy AZ31B tubular workpiece with an outer diameter of 22 mm, a length of 134 mm and a wall thickness of 1.5 mm, and die components were modelled as the rigid-viscoplastic and elastic materials, respectively, with their thermal properties given in Table 1. The von-Mises flow criterion and flow-stress properties of Mg alloy AZ31B according to the Eq. (6) were employed as the material deformation behaviour computation. An average 0.25 Coulomb friction factor was added at the contact surfaces between the tubular workpiece and die cavity. Table 2 is the summary of the simulation conditions.

The constant die-core temperature (T_D) was assigned to the top die, bottom die, outer die core and inner die, when the initial temperature of the tubular workpiece and temperature relief collets was 20 °C (i.e., the room temperature). There were four T_D of 275, 300, 325 and 350 °C and preheating times of material after die closing (t_d) of 10, 20, 30 and 40 s, and thus sixteen heat-transfer simulations for workpieces under non-isothermal conditions were implemented. The THF process simulation was then carried out for each condition under the same loading path and selected axial-feeding rate, as shown in Fig. 7, where the maximum internal pressure was determined by Eq. (3) and the average material temperature. Eventually, the corresponding experimental work for verification was performed with the setup presented in Fig. 8.

5. Results and discussions

All sixteen FE simulation of THF Mg alloy AZ31B barrel-shaped components with different combinations of T_D and t_d were carried out. Fig. 9

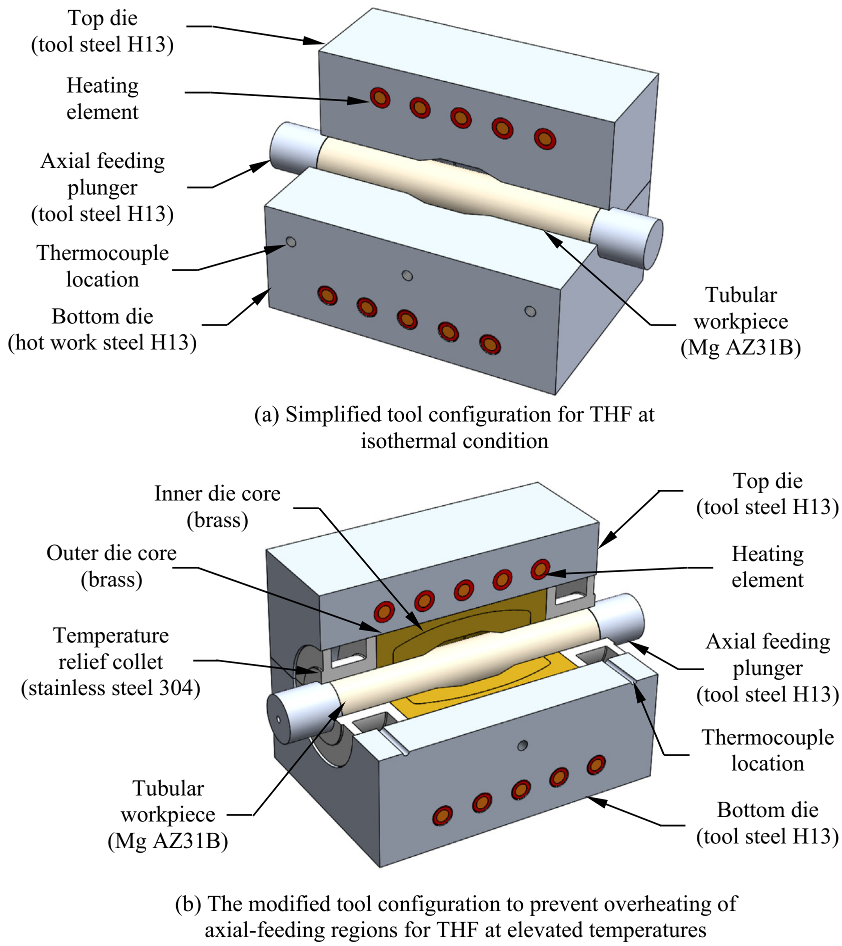

Fig. 5. The difference between the designs of simplified and modified tool configurations for THF at elevated temperatures.

shows the average temperatures of the axial-feeding and deformation regions of the tubular workpiece in different trials, as well as their thermal potential differences upon the THF. The increase of individual T_D or t_d also increased the average temperatures of the axial-feeding and deformation regions, whereas the effect of T_D was more significant. By using the proposed tool design with the temperature relief collets, the thermal potential difference between these two regions was quite remarkable. Each average difference divided by the corresponding T_D was nearly the same, i.e., 27%. Thus, the stability of non-isothermal condition was assured substantially. The values of thermal potential differences decreased steadily when t_d was increased. At the higher T_D (i.e., 350 °C), the difference was reduced greatly, but it was still larger than that in the situation of T_D being less than 350 °C. In other words, to establish a higher thermal potential difference for the improvement of formability at the deformation region and prevention of overheating at the axial-feeding region, T_D could be increased to the value that the

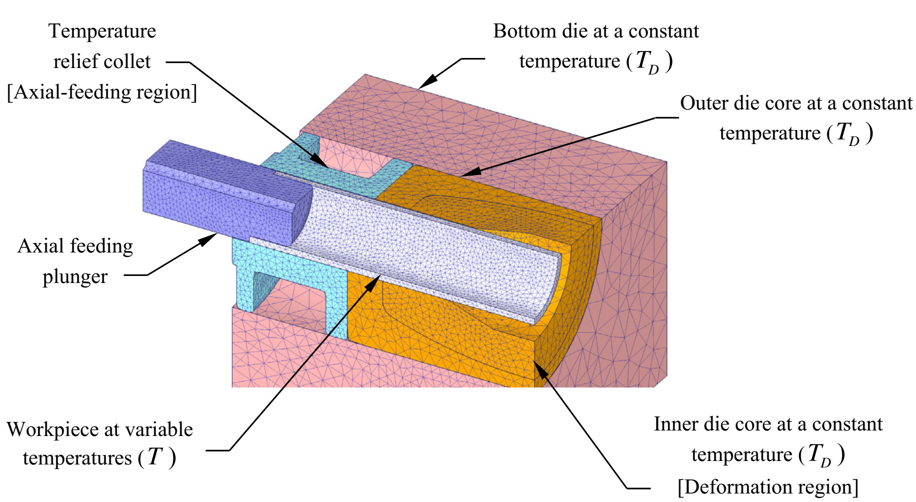

Fig. 6. The 3D model of THF setup for FE simulation having thermal effects.

Table 1
The thermal properties of materials for FE simulation.

Material	Thermal conductivity (W/m·K)	Heat capacity (J/g·K)	Emissivity
Mg alloy AZ31B	96	1.02	0.2
Stainless steel 304	20	0.38	0.3
Brass	122	0.38	0.2
Tool steel H13	24	0.40	0.3

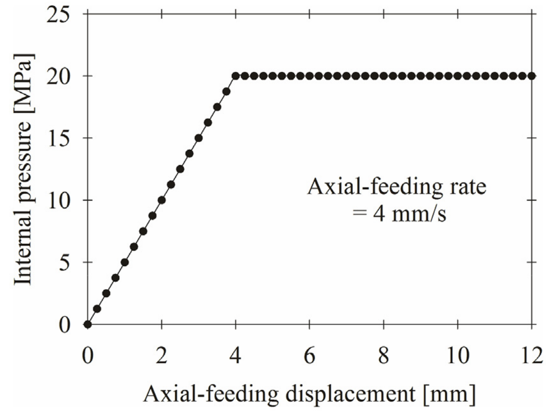

Fig. 7. The loading path used in the THF simulation.

die material and forming media can withstand. Normally, 350 °C was the maximum value of T_D when the thermal-resistant oil was used as the forming medium in THF. Nitrogen or other inert gases would be the alternative if T_D was higher than 350 °C.

Although the increase of Mg alloy AZ31B temperature could improve its formability and elongation, the tubular material still fractured during over-expansion. According to the self-experimental data and literature on the constitutive and fracture behaviours of AZ31B under a wide range of strain rates and temperature conditions [29,30], the elongation before fracture of AZ31B at 250 to 300 °C was around 20%. In the THF, apart from the wrinkling defects, wall thinning usually occurred in the deformation region. When the wall thickness of the tubular workpiece was reduced by a percentage that was larger than the limit of material elongation, the workpiece would tend to fracture, resulting in a failed outcome. Fig. 10 shows the simulation results of THF barrel-shaped components with different combinations of T_D and t_d. Trials 08, 10, 11, 12, 14, 15 and 16 failed because the wall thicknesses of their workpieces were all reduced by more than 20%, fractures might occur easily in this situation. The main cause was that the temperature of their deformation regions was raised over the period and the wall thickness was reduced by the internal pressure at the early stage of the THF process. Comparatively, the temperatures of the deformation regions of Trials 04, 06 and 07 were decreased slightly, and the wall thinning effect was thus moderated. On the other hand, without the wall thinning problem, more serious wrinkling defects were found in Trials 01, 05 and 09, as they were preheated for 10 s only. The temperatures of their deformation regions were around 200 and 250 °C, in which the maximum internal pressure of 20 MPa was insufficient to compensate the total radial stress during the bulging of material. When the T_D was increased, the wrinkling effect was declined gradually. Besides, the wrinkling defects in Trial 02 was relatively small as the temperature of its deformation region was higher. Therefore, the proposed tool design had provided the non-isothermal condition that effectively mitigated the wrinkling effects at the higher temperature under an isothermal condition mentioned in previous section.

The satisfactory THF barrel-shaped components were obtained in Trials 03 and 13, in which the wall thinning of the component in Trial 13 was slightly greater that in Trials 03 (i.e., 13% vs. 9%), because the higher temperature was distributed at the deformation region of Trial 13. Based on the simulation results, the corresponding experiments were carried out for verification. Fig. 11 shows the results of the actual satisfactory and failed barrel-shaped components. The failed component was taken from the process at T_D between 275 and 300 °C, and t_d = around 10 s such that the serious wrinkling defects occurred when the plungers kept pushing the material toward the deformation region. The shape of the satisfactory component was close to the result predicted by the simulation of Trial 13 that thus confirmed the accuracy and reliability of the FE simulation.

Eventually, with the same approach, the Mg alloy AZ31B bike-frame components with 2 mm wall thickness including top tube, down tube, and seat tube were trial-produced by the self-developed 2500-ton hydroforming system and THF dies with the modified collet-type device design, as shown in Fig. 12. To reduce the friction between the workpiece and die surfaces, a water-solvable type warm-forming lubricant W-400 was spread over the surfaces of the die cavity. The seat tube shown in Figs. 12 and 13 was selected as the example for discussions. Likewise, when the T_D and/or the temperature of deformation region of the workpiece were insufficient, the wrinkling defects occurred easily, subject to the maximum internal pressure was being limited for the prevention of the tube fracture. Use of the collet-type device design prevented the axial-feeding region from being overheated. The satisfactory wrinkle-free Mg alloy AZ31B non-axisymmetric tubular seat-tube component was hydroformed successfully under the suitable non-isothermal condition and an appropriate pre-heating time, i.e., $T_D \approx$ 350 °C and $t_d \approx$ 10 s.

6. Conclusions

This paper has provided a theoretical analysis to describe how the temperature of tubular material affected the formation of wrinkling

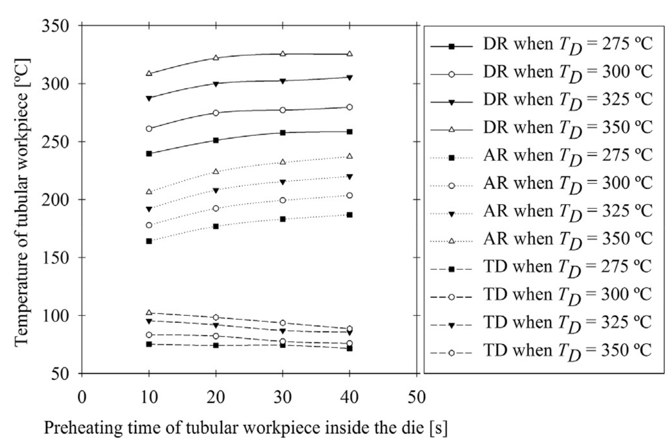

Fig. 8. The experimental setup for THF Mg alloy AZ31B barrel-shaped components at elevated temperatures.

Table 2
The summary of simulation conditions.

Simulation parameter	Value/setting
Number of elements of the tubular workpiece (1/8)	17,397
Iteration method	Direct method
Deformation solver	Sparse
Temperature solver	Sparse
Coulomb friction factor for workpiece/die interface	0.25
Heat-transfer coefficient between each object	11 $MW/m^2 \cdot K$
Constant temperature of die and core die (T_d)	275/300/325/350 °C
Initial temperature of workpiece and collets	20 °C
Axial-feeding stroke	12 mm
Axial-feeding rate	4 mm/s
Preheating time of workpiece in a closed die (t_d)	10/20/30/40 s

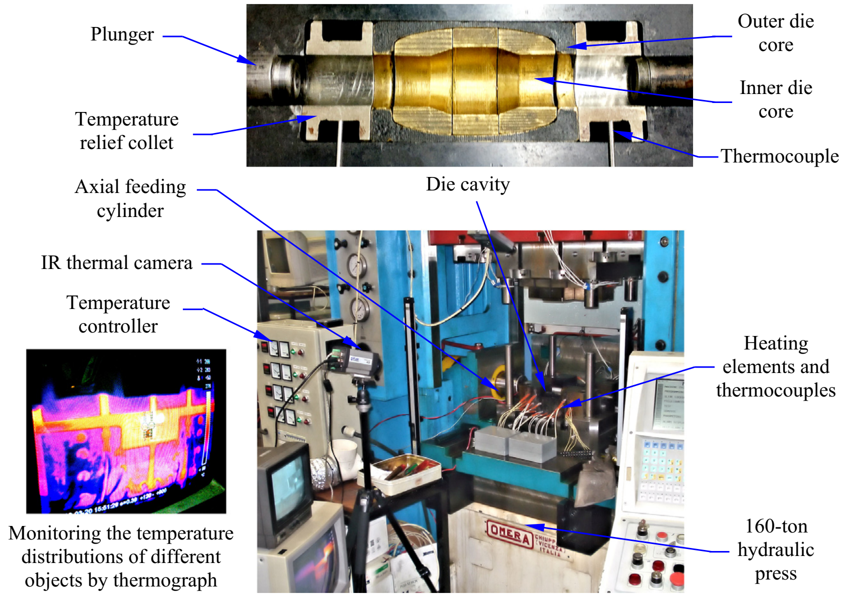

Fig. 9. The average temperatures of the axial-feeding region (AR) and deformation region (DR) as well as the thermal potential difference (TD) of the Mg alloy AZ31B tubular workpiece at different preheating time (t_D) and die-core temperature (T_D).

defects in THF at elevated temperatures. Under the isothermal condition, the increase in temperature decreased the critical wrinkling stress that the wrinkling defects would occur easily. In order to overcome this problem, a breakthrough in tool design was proposed, through the appropriate control of temperature distribution of the Mg alloy AZ31B tubular material. The cost-effective, simple and user-friendly collet-type device design effectively provided the non-isothermal condition for THF, an axisymmetric barrel-shaped component, as the prime example. FE simulation was used to investigate the effects of T_D and t_D on the thermal potential difference between the axial-feeding and deformation

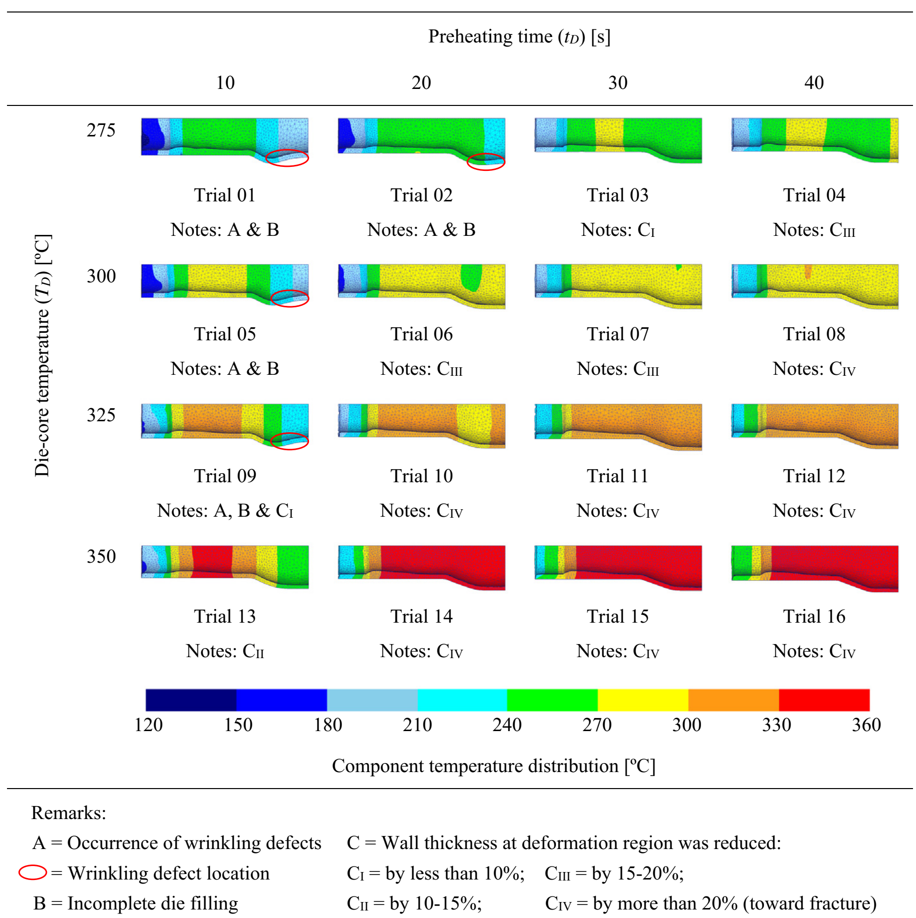

Fig. 10. The simulation results of THF barrel-shaped components with different. combinations of T_D and t_d.

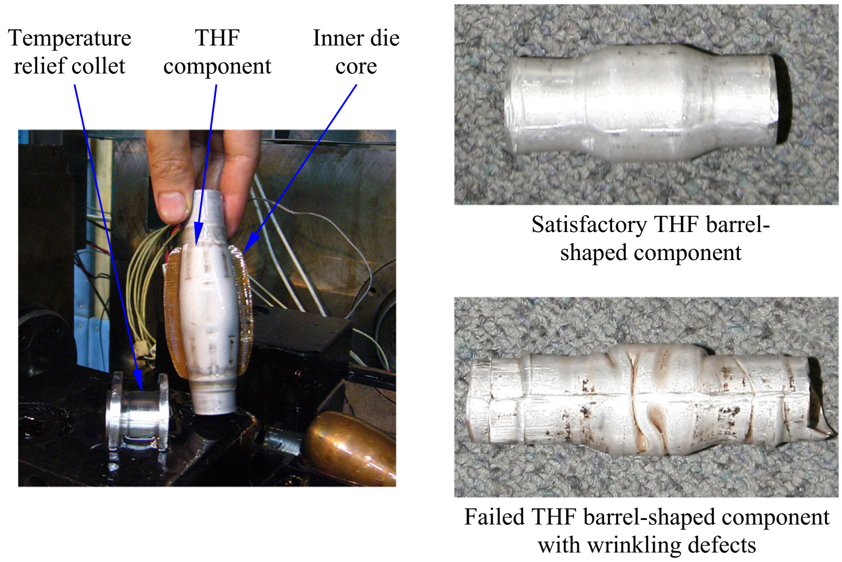

Fig. 11. The experimental outcomes of different THF Mg alloy AZ31B components.

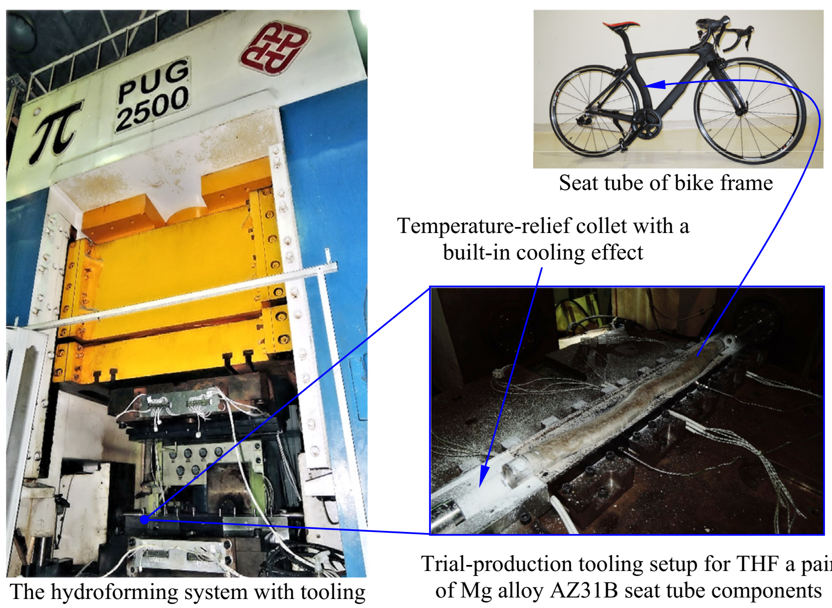

Fig. 12. The self-developed 2500-ton hydroforming system and the trial-production tooling setup for THF Mg alloy AZ31B bike-frame component.

regions, wrinkling occurrence as well as the wall thinning to the THF components. The average temperatures of the axial-feeding and deformation regions were raised by the increase of T_D or t_d, where the effect of T_D was more significant. When the temperature of the deformation region was insufficient, the wrinkling defects were found in the formed components. However, the wall thinning problems leading to the

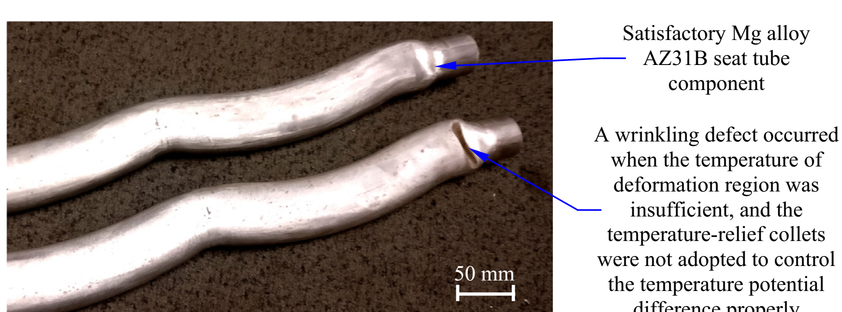

Fig. 13. The Mg alloy AZ31B bike-frame components fabricated by THF at elevated temperatures.

material fracture appeared when the deformation region was overheated. Therefore, the suitable T_D or t_d had to be determined carefully using the FE simulation. The results showed that the satisfactory actual component could be obtained when $T_D \approx 350$ °C and $t_d \approx 10$ s, where the average temperatures of axial-feeding and deformation regions were around 240 and 330 °C, respectively. Finally, with the same approach, a wrinkle-free non-axisymmetric tubular bike-frame component was hydroformed successfully as a more realistic and practical application example.

CRediT authorship contribution statement

T.F. Kong: Methodology, Formal analysis, Investigation, Data curation, Writing - original draft, Writing - review & editing, Visualization. **X.Z. Lu:** Formal analysis, Investigation, Data curation, Writing - review & editing. **L.C. Chan:** Conceptualization, Supervision, Resources, Project administration, Funding acquisition.

Acknowledgments

The work described in this paper was partially supported by the Innovation and Technology Fund (ITF) from the Innovation and Technology Commission of the Government of the Hong Kong Special Administrative Region under project codes: ITS/337/14FX (ZM1T) and ITS/363/15FX (ZM1Y).

Data availability

The raw/processed data required to reproduce these findings cannot be shared at this time due to the non-disclosure agreements with industrial sponsors.

References

[1] W. Liu, Y.Z. Chen, G. Liu, X.L. Cui, Welded double sheet hydroforming of complex hollow component, Trans. Nonferrous Metals Soc. China 22 (2012) s309–s314.
[2] A. Barabi, A. Zarei-Hanzaki, H. Abedi, A. Anoushe, J.H. Cho, The correlation of macro-structure, microstructure, and texture with room temperature mechanical properties of a twinning-induced plasticity automotive steel after friction stir spot welding/processing, Steel Res. Int. 89 (2018), 1800245.
[3] J. Jeswiet, M. Geiger, U. Engel, M. Kleiner, M. Schikorra, J. Duflou, R. Neugebauer, P. Bariani, S. Bruschi, Metal Forming Progress Since 2000, CIRP-JMST 1 (2008) 2–17.
[4] A. Alaswad, K.Y. Benyounis, A.G. Olabi, Tube hydroforming process: a reference guide, Mater. Des. 33 (2012) 328–339.
[5] M. Koc, T. Altan, An overall review of the tube hydroforming (THF) technology, J. Mater. Process. Technol. 108 (2001) 384–393.
[6] T. Zribi, A. Khalfallah, H. BelHadjSalah, Experimental characterization and inverse constitutive parameters identification of tubular materials for tube hydroforming process, Mater. Des. 49 (2013) 866–877.
[7] R. Bihamta, G. D'Amours, Q.H. Bui, M. Guillot, A. Rahem, M. Fafard, Numerical and experimental studies on the new design concept of hydroforming dies for complex tubes, Mater. Des. 47 (2013) 766–778.
[8] E. Ghassemieh, Materials in automotive application, state of the art and prospects, New Trends and Developments in Automotive Industry, InTech, 2011.
[9] A. Kocańda, H. Sadłowska, Automotive component development by means of hydroforming, Arch. Civ. Mech. Eng. 8 (2008) 55–72.
[10] M. Tolazzi, Hydroforming applications in automotive: a review, Int. J. Mater. Form. 3 (2010) 307–310.
[11] Y. Cai, X.S. Wang, S.J. Yuan, Pre-form design for hydro-forming of aluminum alloy automotive cross members, Int. J. Adv. Manuf. Technol. 86 (2016) 463–473.
[12] J. Zhang, S. Yan, H. Qu, Recent progress in magnesium hydride modified through catalysis and nanoconfinement, Int. J. Hydrog. Energy 43 (2018) 1545–1565.
[13] H. Jafari, E. Heidari, A. Barabi, M. Dashti Kheirabadi, Effect of phase transformation during long-term solution treatment on microstructure, mechanical properties, and bio-corrosion behavior of Mg–5Zn–1.5 Y cast alloy, Acta Metall. Sin. 31 (2018) 561–574.
[14] A.S. Anoushe, A. Zarei-Hanzaki, H.R. Abedi, A. Barabi, C. Huang, F. Berto, On the microstructure evolution during isothermal low cycle fatigue of β-annealed Ti-6242S titanium alloy: internal damage mechanism, substructure development and early globularization, Int. J. Fatigue 116 (2018) 592–601.
[15] S.H. Zhang, K. Zhang, Y.C. Xu, Z.T. Wang, Y. Xu, Z.G. Wang, Deep-drawing of magnesium alloy sheets at warm temperatures, J. Mater. Process. Technol. 185 (2007) 147–151.
[16] D.G. Tari, M.J. Worswick, S. Winkler, Experimental studies of deep drawing of AZ31B magnesium alloy sheet under various thermal conditions, J. Mater. Process. Technol. 213 (2013) 1337–1347.
[17] D.G. Tari, M.J. Worswick, Elevated temperature constitutive behavior and simulation of warm forming of AZ31B, J. Mater. Process. Technol. 221 (2015) 40–55.
[18] H.K. Yi, E.J. Pavlina, C.J. Van Tyne, Y.H. Moon, Application of a combined heating system for the warm hydroforming of lightweight alloy tubes, J. Mater. Process. Technol. 203 (2008) 532–536.
[19] G. Liu, W.D. Zhang, Z.B. He, S.J. Yuan, Z. Lin, Warm hydroforming of magnesium alloy tube with large expansion ratio within non-uniform temperature field, Trans. Nonferrous Metals Soc. China 22 (2012) s408–s415.
[20] L.F. Yang, C. Guo, A simple experimental tooling with internal pressure source used for evaluation of material formability in tube hydroforming, J. Mater. Process. Technol. 180 (2006) 310–317.
[21] N. Abedrabbo, M. Worswick, R. Mayer, I. van Riemsdijk, Optimization methods for the tube hydroforming process applied to advanced high-strength steels with experimental verification, J. Mater. Process. Technol. 209 (2009) 110–123.
[22] J.Y. Park, S.W. Han, H.S. Jeong, J.R. Cho, Y.H. Moon, Advanced sealing system to prevent leakage in hydroforming, J. Mater. Process. Technol. 247 (2017) 103–110.
[23] G. Liu, J.Y. Peng, S.J. Yuan, B.G. Teng, K. Li, Analysis on critical conditions of sidewall wrinkling for hydroforming of thin-walled tee-joint, Int. J. Mach. Tools Manuf. 97 (2015) 42–49.
[24] J. Cao, X. Wang, An analytical model for plate wrinkling under tri-axial loading and its application, Int. J. Mech. Sci. 42 (2000) 617–633.
[25] H. Watanabe, H. Tsutsui, T. Mukai, M. Kohzu, S. Tanabe, K. Higashi, Deformation mechanism in a coarse-grained Mg–Al–Zn alloy at elevated temperatures, Int. J. Plast. 17 (2001) 387–397.
[26] Q.F. Chang, D.Y. Li, Y.H. Peng, X.Q. Zeng, Experimental and numerical study of warm deep drawing of AZ31 magnesium alloy sheet, Int. J. Mach. Tools Manuf. 47 (2007) 436–443.
[27] L.C. Chan, X.Z. Lu, Material sensitivity and formability prediction of warm-forming magnesium alloy sheets with experimental verification, Int. J. Adv. Manuf. Technol. 71 (2014) 253–262.
[28] W.T. Jia, S. Xu, Q.C. Le, L. Fu, L.F. Ma, Y. Tang, Modified fields–Backofen model for constitutive behavior of as-cast AZ31B magnesium alloy during hot deformation, Mater. Des. 106 (2016) 120–132.
[29] F. Feng, S.Y. Huang, Z.H. Meng, J.H. Hu, Y. Lei, M.C. Zhou, Z.Z. Yang, A constitutive and fracture model for AZ31B magnesium alloy in the tensile state, Mater. Sci. Eng. A 594 (2016) 334–343.
[30] F. Feng, S.Y. Huang, Z.H. Meng, J.H. Hu, Y. Lei, M.C. Zhou, Z.Z. Yang, Experimental study on tensile property of AZ31B magnesium alloy at different high strain rates and temperatures, Mater. Des. 57 (2014) 10–20.